# On the Mathematical Theory of the Linearly-Graded P-N Junction\*

**Abstract:** This paper presents a numerical analysis of the mechanisms of operation within a linearly-graded p-n junction. Considered in this analysis are three important modes of junction operation: equilibrium, forward bias, and reverse bias in the collector junction. In addition, calculations of electrical space-charge layer capacitance are presented for the forward-biased linearly-graded junction. The conclusions derived are compared, in graphical form, with the results of previous investigations of the linearly-graded junction.

### Introduction

In his theory of p-n junctions in semiconductors, Shockley<sup>1</sup> presented the first mathematical analysis applicable to structures containing a linearly-graded impurity atom distribution. The Shockley analysis was based upon the simplifying assumption that the space-charge layer of a linearly-graded junction is completely depleted of mobile charge carriers. This assumption eliminates from Poisson's equation the distribution terms for mobile holes and electrons, and thereby reduces a difficult system of differential equations to a single, mathematically tractable differential equation. Despite this simplifying assumption, many conclusions derived from the depletion layer approximation were subsequently verified by laboratory experiment. For this reason, the depletion layer theory of a linearly-graded p-n junction is an important part of the semiconductor literature.

Shockley's depletion layer theory contains restrictive features rendering it inapplicable to several important modes of junction operation. In particular, to assume that the space-charge layer is free of mobile charge carriers is to imply that his theoretical approximation is not applicable to forward-biased p-n junctions, nor to reverse-biased junctions containing a large electric current density (such as the collector in a transistor). Although these limitations of the depletion layer theory have been recognized by many workers, a rigorous analytical treatment of the problem has not been reported. Instead, other approaches have been used to simplify the mathematical equations characterizing a semiconductor junction; each

In Shockley's treatment, an estimate was made concerning the influence of mobile electrons and holes upon the space-charge layer characteristics of a linearly-graded junction. This estimate was limited to structures at thermal and potential equilibrium. Shockley established that near charge neutrality can be mathematically obtained within the transition region\* of a linearly-graded junction containing a small impurity atom gradient. In this type of junction, the space-charge layer modifications arising from mobile holes and electrons were estimated by comparing the space-charge electrical capacitance of a linearly-graded *p-n* junction with the capacitance of one exhibiting near charge neutrality.

For a linearly-graded junction, Morgan and Smits<sup>2</sup> obtained numerical solutions of the complete Poisson's equation, including the charge distribution arising from mobile holes and electrons. Although their investigation was conducted with the aid of a computer, they eliminated many mathematical difficulties by assuming a zero electric current, even for a forward-biased junction. This particular treatment of the linearly-graded junction problem has been severely criticized in the literature.<sup>3</sup> The basis of this criticism is that by neglecting the influence of an electric current within a forward-biased linearly-graded junction, the Morgan and Smits analysis is inapplicable at

approach, however, has introduced a new set of uncertainties concerning the analytical limitations arising from the use of simplifying assumptions.

<sup>♦</sup> The analysis presented in this paper was supported in part by the Air Force Cambridge Research Laboratories, Office of Aerospace Research, under Contract AF19(628)-5072, Project 4608.

<sup>\*</sup> Throughout this discussion, the transition point of a one-dimensional  $p \cdot n$  junction is defined as the location at which the predominant type of impurity atom changes from donor to acceptor. Similarly, the transition region of a  $p \cdot n$  junction represents that portion of the semiconductor material in the immediate vicinity of the  $p \cdot n$  junction transition point.

moderate and large values of forward biasing voltage. We show below that this criticism may not be justified over most of the useful range of forward bias.

In a later treatment of the linearly-graded junction problem, Sah<sup>3</sup> obtained an analytical approximation for the solution of Poisson's equation containing an electrostatic charge due both to ionized impurity atoms and to mobile charge carriers (holes and electrons). The principal difference between the analysis of Sah and the analysis of Morgan and Smits lies in their respective methods for solving this non-linear differential equation. Sah applied Picard's Algorithm,<sup>4,5</sup> obtaining only the first approximation from a recurrence relation for the solution of this differential equation; Morgan and Smits obtained their solution by numerical methods.

In this paper the analysis is based upon information derived from numerical solutions of the complete set of differential equations characterizing a linearly-graded p-n junction. The system of equations used in this analysis was previously outlined by Van Roosbroeck<sup>6</sup> in connection with his investigations of the flow of electrons and holes in semiconductor materials. By combining this large number of equations, it can be shown that a set of three simultaneous non-linear differential equations describes the operation of a p-n junction. Finite difference methods have been used to solve this set of equations, with the aid of an electronic computer.

Although numerical techniques do not provide explicit equations describing the physical and electrical properties of a linearly-graded junction, such information has been obtained in an indirect fashion. From a series of computer calculations, parameters normally described by mathematical formula are presented in a graphical form; thereby, information derived from the present investigation is readily available for semiconductor device design.

### List of definitions

- Conized impurity atom gradient
- C Electrical capacitance
- C(x) Ionized impurity atom distribution
- $D_n$  Diffusion constant for electrons
- $D_p$  Diffusion constant for holes
- E Electric field
- $J_n$  Electric current density due to electrons
- $J_p$  Electric current density due to holes
- $J_T$  Total electric current density
- $K_0$  A dimensionless variable
- $\mathfrak{L}_{D}$  Debye shielding distance
- $\Re_n(x)$  Recombination rate for electrons
- $\Re_{p}(x)$  Recombination rate for holes
- U Dimensionless electrostatic potential variable
- V<sub>a</sub> Applied junction biasing voltage
- $V_D$  Equilibrium diffusion voltage of a p-n junction
- $V_T$  Total p-n junction voltage  $(V_D + V_a)$

- W Electrostatic energy
- n(x) Mobile electron distribution
- p(x) Mobile hole distribution
- q Electron charge
- x A spatial variable
- $x_n$  Space-charge layer boundary in n-type material
- $x_p$  Space-charge layer boundary in p-type material
- y Dimensionless spatial variable
- $\epsilon_0$  Permittivity of free space
- κ Dielectric constant
- $\mu_n = D_n q/kT$
- $\mu_p = D_p q/kT$
- $\varphi_n$  Quasi-Fermi level for electrons
- $\varphi_p$  Quasi-Fermi level for holes
- $\psi$  Electrostatic potential

### **Analysis**

In a homogeneous semiconductor, the steady-state hole and electron distributions [p(x)] and n(x) are described by the equations

$$\frac{d^2\psi(x)}{dx^2} = -\frac{q}{\kappa\epsilon_0} \left[ C(x) - n(x) + p(x) \right], \qquad (1a)$$

$$J_p(x) = -q D_p \frac{dp(x)}{dx} - q \mu_p p(x) \frac{d\psi(x)}{dx}, \qquad (1b)$$

$$J_n(x) = q D_n \frac{dn(x)}{dx} - q \mu_n n(x) \frac{d\psi(x)}{dx}, \qquad (1c)$$

$$0 = \Re_p(x) - \frac{1}{a} \frac{dJ_p(x)}{dx}, \tag{1d}$$

$$0 = \Re_n(x) - \frac{1}{a} \frac{dJ_n(x)}{dx} , \qquad (1e)$$

$$J_T(x) = J_p(x) + J_n(x), (1f)$$

assuming no trapping mechanisms within the material under consideration.

Equation (1a) is Poisson's equation, which relates the divergence of the electric field  $[E(x) = -d\psi(x)/dx]$  to the total electrostatic charge due to both mobile charge carriers [p(x)] and [p(x)] and ionized impurity atoms [p(x)]. For a linearly-graded [p-n] junction, the net ionized impurity atom distribution is described by the relation

$$C(x) = \mathfrak{A}_0 x, \tag{2}$$

where  $\alpha_0$  is the concentration gradient of these ionized impurity atoms.

Equations (1b) and (1c) give the electric current densities within a semiconductor  $(J_p, J_n)$  arising from the transport of mobile holes and electrons. These equations are fundamentally the same as those of M. Smoluchowski, rewritten for hole and electron transport. They express the dependency of each electric current component  $(J_p \text{ and } J_n)$  upon the concentration gradients of holes and electrons,

253

the mobility of these charge carriers, and the electrostation obtained at each nodal location. Thereafter, potential gradient (electric field) within a semiconduct using a finite-difference form for the three differential

For simplicity, the hole and electron mobilities  $(\mu_p, \mu_n)$ , and the hole and electron diffusion constants  $(D_p, D_n)$ , are often assumed invariant within a particular sample of semiconductor material. This, of course, is sometimes an unreasonable simplification. Experiment shows that within a given sample of semicondictor material, the mobilities and diffusion constants of holes and electrons often undergo large changes. Such changes arise at large values of electric field and at large values of impurity atom concentration. For this reason, the present paper considers the influence of both electric field and impurity atom density upon the mobility and diffusion properties of holes and electrons.

Equations (1d) and (1e) are the continuity equations for holes and electrons exhibiting an unspecified mechanism for recombination. To avoid introducing specific recombination and generation mechanisms, these equations will be simplified by completely neglecting such mechanisms from the present analysis of a linearly-graded junction; this is equivalent to assuming an infinite lifetime for holes and electrons. Infinite minority carrier lifetimes may appear to introduce severe limitations upon the applicability of the present analysis, but this is not the case. The influence of carrier generation upon p-n junction operation is adequately considered in the literature. <sup>14</sup> Furthermore, in the present analysis the minority carrier sink usually provided by bulk recombination is replaced by a sink at the semiconductor boundary; thereby, a forward-biased junction of infinite carrier lifetime will exhibit an electric

Equation (1f) states that the total electric current density  $(J_T)$  is the algebraic sum of electric current due to both holes  $(J_p)$  and electrons  $(J_n)$ .

The six equations (1) can be combined into three simultaneous non-linear differential equations in three variables: electrostatic potential, mobile hole concentration, and mobile electron concentration. A rigorous mathematical solution of the p-n junction problem requires that this set be solved. Such a solution is a difficult task; in fact, an attempt to solve this problem by traditional analytical means will probably end in failure. It appears reasonable to assume that there exists no rigorous analytical solution for this system of equations, and other means must therefore be used in a mathematical investigation of the junction problem.

The analysis presented in this paper is the result of a numerical solution of the mathematical equations (1). Three one-dimensional nodal arrays, each composed of up to five thousand spatial locations, are used to represent the junction under consideration. Boundary conditions for each independent variable, in addition to the impurity atom distribution, are introduced as constraints upon the

olutions obtained at each nodal location. Thereafter, using a finite-difference form for the three differential equations, relaxation techniques are applied sequentially to the three matrix arrays; this leads to solutions for specific *p-n* junction problems. Because numerous texts are available on the relaxation solution of partial differential equations, <sup>5-19</sup> details concerning the method are not repeated here.

For a linearly-graded p-n junction, the literature contains four different approximation methods for the solution of the system of differential equations. As previously stated, the Shockley solution is based upon an assumption that the structure under consideration is depleted of holes and electrons. Morgan and Smits obtained a numerical solution, although they assumed an electric current of zero; this simplification eliminates two of the three non-linear differential equations. Sah used the same simplification introduced by Morgan and Smits, and thereafter obtained an approximate analytical solution for the differential equation characterizing a linearly-graded p-n junction. Both of these solutions are directed toward the analysis of a forward-biased junction. In contrast, Kirk<sup>20</sup> investigated the abrupt collector junction at large values of collector current, and thereafter suggested the applicability of this model to diffused type structures. Kirk's study was intended to establish the more general properties of a collector junction, and for this reason no attempt was made to solve the mathematical problem in a rigorous fashion.

The Morgan and Smits solution assumed that no electric current is present in the structure, even at large values of forward biasing voltage. After introducing this simplification into (1), and writing the hole and electron densities in terms of the quasi-Fermi levels  $\varphi_p$  and  $\varphi_n$ ,

$$n = n_i \exp \left[\frac{q}{kT} (\psi - \varphi_n)\right]$$
, and (3a)

$$p = n_i \exp \left[ \frac{q}{kT} (\varphi_p - \psi) \right], \qquad (3b)$$

one obtains

$$\frac{kT}{q \, \mathbb{I} \, dx^2} = -\frac{\rho(x)}{\kappa \epsilon_0} \,, \tag{4a}$$

$$\frac{d\varphi_n}{dx} = \frac{d\varphi_p}{dx} = 0, \tag{4b}$$

where

$$\rho(x) = q \left\{ C(x) - 2n_i \exp \left[ \frac{q}{2kT} (\varphi_p - \varphi_n) \right] \sinh U \right\}$$
(5)

and

$$U = \frac{q}{kT} \left\{ \psi - \frac{1}{2} (\varphi_p + \varphi_n) \right\}. \tag{6}$$

254

Because the quasi-Fermi levels are assumed constant (zero electric current), the normalized p-n junction electrostatic potential (6) is given by the solution of a single non-linear differential equation (4a). Morgan and Smits solved this problem by step-by-step numerical methods<sup>21</sup> using an electronic computer.

There have been two basic criticisms<sup>3</sup> of the Morgan and Smits analysis: First, the assumption of a zero electric current placed severe limitations upon the applicability of the analysis and, second, the computer solution did not provide analytical equations characterizing junction operation. Thereafter, however, Sah used the same mathematical simplification (zero electric current) used by Morgan and Smits and, after applying Picard's Algorithm to a modified form of Eq. (4a), obtained an approximate analytical solution for this particular boundary value problem.

In principle, there are many differential equations to which the Picard method can be applied, although in practice one is seldom able to complete such a task. If we write Eq. (4a) in the form

$$\frac{d^2 U}{dz^2} = A \sinh U_0 + Bz, \tag{7}$$

a guess can be introduced for  $U_0$ . By solving this differential equation, a first-approximation is obtained for the required solution. The approximate solution is next substituted for  $U_0$  in (7), and this equation is again solved; a better approximation is thereby obtained for the required solution. In theory, after an infinite number of similar iterations, an exact solution will be obtained for this differential equation. It is to be emphasized, however, that in solving a differential equation by the Picard technique, no general method exists whereby one can establish the error resulting from a finite number of iterations.

The complicated nature of this differential equation has prevented an extensive application of Picard's Algorithm. To cope with this difficulty, Sah first introduced the expression<sup>3</sup>

$$U_0 = \xi z, \tag{8}$$

where  $\xi$  is a constant of proportionality. This substitution results in a linear differential equation of elementary form, and thus a solution was readily obtained. A second iteration in this process becomes difficult, if not impossible. For this reason, the solution was limited to a first approximation for the required potential distribution. Thereafter, two guesses were made for a magnitude of the proportionality constant in Eq. (8). The first guess (Approx. 1 in Ref. 3) was assumed inferior to the second guess (Approx. 2 in Ref. 3); it can be shown that this first guess is actually superior, and the resulting electrostatic potential distribution formula is satisfactory for most engineering purposes.

The mathematical investigations of Morgan and Smits, and also those of Sah, introduce important questions concerning the validity of the simplifying assumptions. For example, there is no information concerning the relative error arising from a zero-current analysis of forward biased linearly-graded p-n junctions. Further, the approximate analytical solution obtained by Sah, in conjunction with questions concerning the magnitude of  $\xi$  in Eq. (8), has resulted in a situation for which it is exceedingly difficult to evaluate accurately the relative error arising from the approximation method.

For the reverse-biased collector junction, Kirk<sup>20</sup> assumed that only one type of mobile charge carrier existed within the collector junction space-charge layer. This situation will arise in transistors containing a forward-biased emitter junction. In addition, Kirk restricted his analysis to transistors operating at large values of collector junction biasing voltage. Kirk's restriction results from an assumption that mobile charge carriers maintain a terminal velocity throughout the entire collector junction space-charge layer. With the foregoing assumptions, solving Poisson's equation (1a) is a straightforward problem and is comparable to Shockley's space-charge analysis of linearlygraded p-n junctions. Because there is no experimental evidence indicating that holes exhibit a terminal velocity, p-n-p transistor operation is excluded from Kirk's analysis. Furthermore, it will be shown that electrons can be assumed to be at their terminal velocity only at substantial values of collector junction reverse biasing voltage.

### The equilibrium junction

The initial studies of linearly-graded junction theory were directed toward structures at thermal equilibrium. From Boltzmann statistics, Shockley¹ obtained mathematical equations relating the mobile charge carrier densities (holes and electrons) to the electrostatic potential. Thereafter, these Boltzmann equations were combined with Poisson's equation for a linearly-graded *p-n* junction. Resulting from this combination is a non-linear differential equation that mathematically characterizes the operation of a linearly-graded *p-n* junction at thermal and potential equilibrium,

$$\frac{d^2 U}{dy^2} = \frac{1}{K_0^2} (\sinh U - y), \tag{9}$$

where

$$U = q\psi/kT, (10a)$$

$$y = \alpha_0 x / 2n_i, \tag{10b}$$

$$K_0 = \mathcal{L}_D \Omega_0 / 2n_i$$
, and (10c)

$$\mathcal{L}_D^2 = \kappa \epsilon_0 k T / 2q^2 n_i. \tag{10d}$$

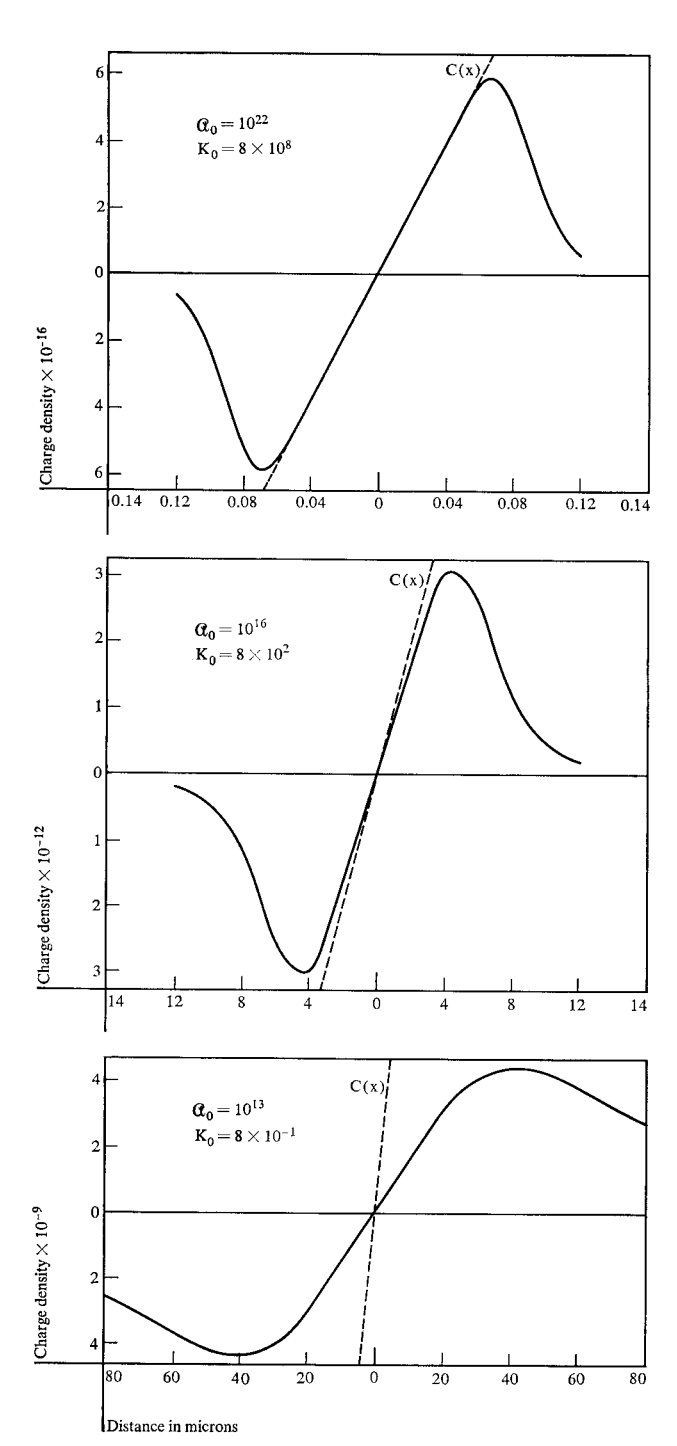


Figure 1 Equilibrium space-charge layer distribution in a linearly-graded silicon p-n junction. (Note change of scale in abscissa.)

Recognizing the inherent difficulties associated with solving Eq. (9), Shockley obtained two limiting approximations for the solution of this equation. He first assumed that the dimensionless parameter  $K_0$  is very small, thereby implying a condition of near charge neutrality throughout

the entire semiconductor structure; charge neutrality reduces Poisson's equation (9) to Laplace's equation. This assumption further implies that the hole and electron densities are everywhere sufficient to neutralize the electrostatic charge arising from both ionized impurity atoms and the thermally-generated mobile charge carriers.

Similarly, Shockley investigated other solutions of Eq. (9), this time assuming that the dimensionless parameter  $K_0$ is indefinitely large. In this situation, Eq. (9) does not reduce to Laplace's equation; instead, this equation retains a large electrostatic charge. From physical arguments, it is readily shown the electrostatic charge in Poisson's equation (9) arises from hole and electron depletion throughout the immediate vicinity of a junction transition point. In this form Eq. (9) is a second-order nonlinear differential equation having no exact analytical solution; approximation methods are therefore necessary. From approximations previously used by Schottky,22 Schottky and Spenke,23 and Mott,24 Shockley eliminated from Eq. (9) the influence of mobile holes and electrons (by removing the term sinh U), thereby obtaining a mathematically tractable boundary value problem.

A more general formulation of the linearly-graded junction problem has now established that the dimensionless parameter  $K_0$  in Eq. (10c) is dependent upon the applied junction biasing voltage.<sup>2</sup> For this reason, it is particularly important to consider the physical meaning of this dimensionless parameter, and the inherent characteristics of linearly-graded p-n junctions at intermediate values of  $K_0$ .

Before discussing the equilibrium *p-n* junction, we shall first consider a basic property of semiconductor material: its tendency to maintain charge neutrality. If throughout a region of semiconductor material the number of holes (electrons) deviates appreciably from the corresponding number of ionized acceptor (donor) atoms, the resulting electrostatic forces will yield a potential energy per hole (electron) that is enormously greater than the mean thermal energy. In this situation, unless special mechanisms are present to support these large differences of potential, the mobile charge carriers will rapidly move in such a way as to restore charge neutrality.

The quantity  $\mathfrak{L}_D$ , defined by Eq. (10d), is called the Debye length (or the Debye shielding distance), since Debye<sup>25</sup> has shown that the electric field of a point charge in an electrolyte varies as  $(1/r) \exp(-r/\mathfrak{L}_D)$ . From his analysis, Debye established that at distances greater than  $\mathfrak{L}_D$  (when  $\mathfrak{L}_D < r$ ), the electric field arising from a point charge is shielded by mobile charges of opposite sign. Whereas the direct application of Debye's equations to semiconductor material is open to question, Debye shielding is certainly a mechanism encountered in linearly-graded junctions.

From Eqs. (10c) and (10d),  $K_0$  is the dimensionless ratio of the Debye shielding distance in a semiconductor

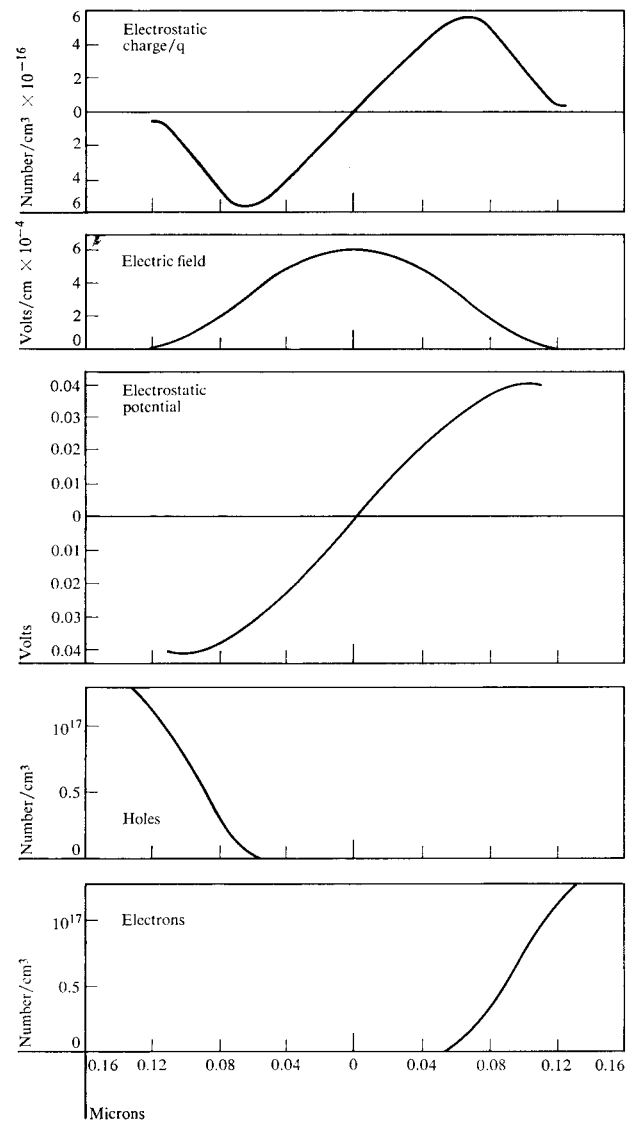


Figure 2 Space-charge layer characteristics of a linearly-graded p-n junction at equilibrium (silicon) ( $K_0 = 8 \times 10^8$ ;  $\alpha_0 = 10^{22}$ ).

 $(\mathfrak{L}_D)$ , and a characteristic length of the impurity atom concentration gradient  $(2n_i/\mathfrak{A}_0)$ . When  $K_0$  is small (small impurity atom gradient), the Debye theory shows that mobile charge carriers (holes and electrons) tend to maintain charge neutrality throughout the semiconductor structure. In contrast, when  $K_0$  is large (large impurity atom gradient) the electric field is sufficient to deplete the semiconductor junction of mobile charge carriers, and thereby establish a well defined space-charge region.

Figure 1 illustrates the calculated equilibrium space-charge distribution for three different linearly-graded p-n junctions at room temperature:  $\mathfrak{A}_0 = 10^{13}$ ,  $10^{16}$ , and  $10^{22}$ , corresponding to  $K_0 = 8 \times 10^{-1}$ ,  $8 \times 10^2$ , and  $8 \times 10^8$ , respectively. This series of calculations was performed by numerical methods, using the differential equations (1).

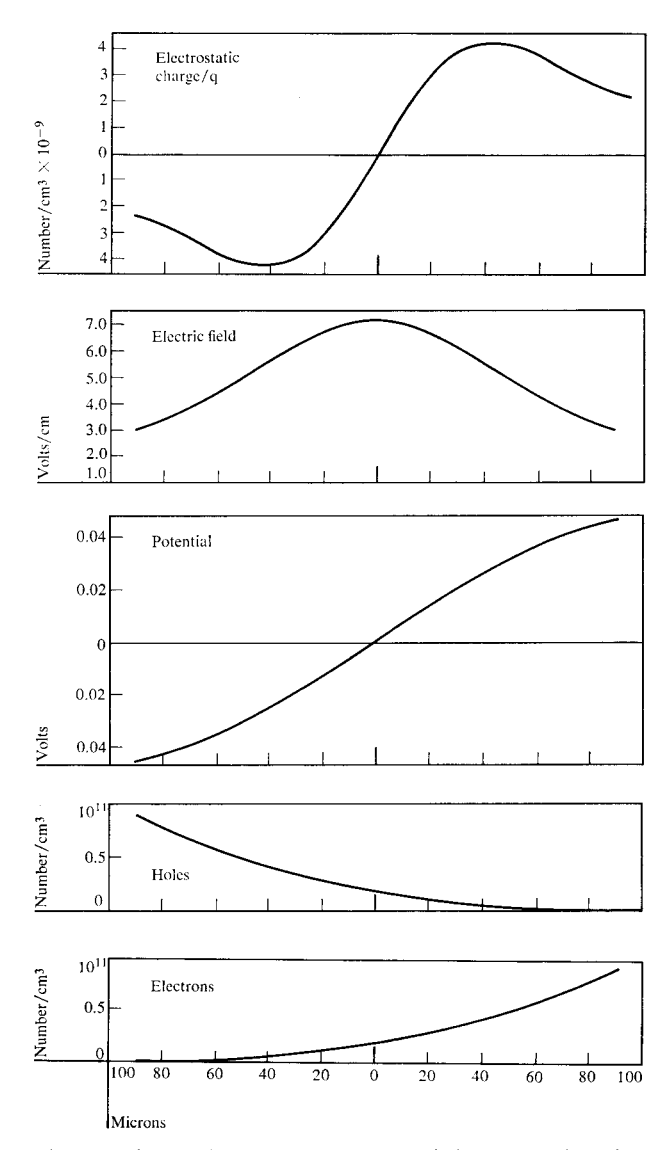
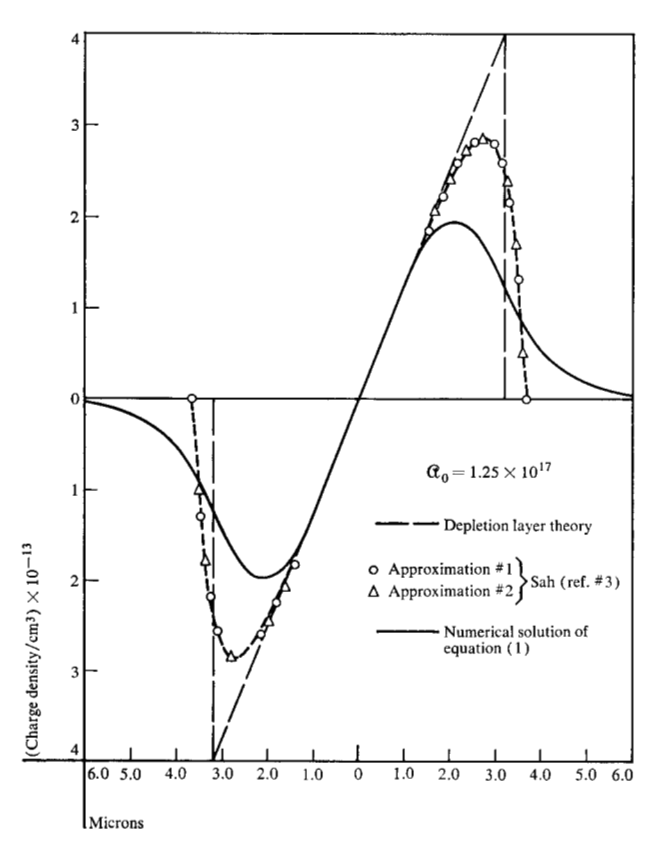


Figure 3 Space-charge layer characteristics of a linearly-graded *p-n* junction at equilibrium (silicon) ( $K_0 = 8 \times 10^{-1}$ ;  $\alpha_0 = 10^{13}$ ).

From Fig. 1, the magnitude of  $K_0$  (as established by the impurity atom gradient) determines the degree of impurity ion neutralization occurring within a p-n junction space-charge region. At large values of impurity atom gradient ( $K_0$  large), the total electrostatic charge density is approximately equal to the density of ionized impurity atoms C(x). In contrast, at small values of impurity atom-gradient ( $K_0$  small), the electrostatic charge density is everywhere smaller than the density of ionized impurity atoms. Although Fig. 1 provides little insight into the mechanism by which charge neutralization arises in a linearly-graded p-n junction, this illustration is qualitatively consistent with the Debye theory for electrostatic shielding.

Further insight into the mechanisms of charge neutralization can be obtained from Figs. 2 and 3. At large values



**Figure 4** Calculated space-charge distribution within a linearly-graded *p-n* junction.

of impurity atom gradient ( $\alpha_0 = 10^{22}$  atoms/cm<sup>4</sup>) the space-charge layer is substantially free of mobile charge carriers (holes and electrons), and therefore the entire electrostatic charge arises from ionized impurity atoms (Fig. 2). In contrast, at small values of impurity atom gradient (Fig. 3) the space-charge electric field is insufficient to cause hole and electron depletion. Clearly, from the Debye theory, structures containing a small impurity atom gradient ( $K_0$  small) also contain large quantities of majority carriers within each side of the space-charge layer (electrons in the *n*-type region and holes in the *p*-type region), and these mobile charge carriers partially neutralize the electrostatic charge arising from ionized impurity atoms.

In this discussion of Shockley's analysis, we next direct our attention to equilibrium junctions containing a well defined space-charge region ( $K_0$  large). As previously stated, Shockley assumed this type of structure was completely depleted of mobile holes and electrons, and thereby reduced Eq. (9) to a tractable differential equation. This simplifying assumption has one obvious difficulty: by eliminating the mobile charge carrier terms from Poisson's equation, Shockley also removed from this equation any mechanism by which the space-charge layer could ter-

minate upon charge-neutral semiconductor material. For this reason, to mathematically approximate the mechanism of space-charge layer termination Shockley was forced to adopt an artifical set of space-charge layer boundary conditions.

From Shockley's simplified form of Poisson's equation, physical arguments can be used to show that the space-charge electric field is maximum at the junction transition point, and that this field decreases with distance into both the *n*-type and *p*-type semiconductor material. At specific locations this electric field becomes zero, and thereafter it changes sign and increases in magnitude to infinity. At these points of zero electric field Shockley assumed that the space-charge layer terminates, and he mathematically represented this boundary by an abrupt transition from Poisson's equation to Laplace's equation. The result of this simplifying assumption is a discontinuous termination of the space-charge in both the *n*-type and *p*-type semiconductor material.

Figure 4 provides a comparison between several different calculations of the equilibrium space-charge distribution within a linearly-graded *p-n* junction. This illustration shows that the depletion layer method yields only a crude approximation. Further, Fig. 4 also shows that although the Sah solution is an improvement over the depletion layer concept, that solution is also an imprecise approximation. Finally, numerical calculations from the Morgan and Smits analysis are found to be in substantial agreement with a numerical solution of Eqs. (1); their computation of the space-charge distribution can thus be considered accurate and free of unnecessary approximations.

Before further comparisons are made among these theoretical methods, it is first necessary to define a location for the termination of each type of mathematically calculated space-charge layer. In the depletion layer theory this question offers little difficulty because Shockley's discontinuous termination provides a well-defined boundary. In contrast, Sah assumed that charge neutrality represented an outer boundary for a p-n junction space-charge layer. From Fig. 4, it is clear that Sah's calculation of the equilibrium space-charge width yields a magnitude slightly greater than the value given by the depletion layer theory. Throughout the present investigation, the space-charge layer is assumed to be terminated at locations where the electrostatic charge density is one-half its maximum value on each side of the structure. In most practical situations, this defined location for the space-charge layer boundary is in substantial agreement with other investigations of the linearly-graded junction problem.

From these arbitrary definitions for the space-charge layer boundaries, Fig. 5 presents the calculated space-charge layer width using three different methods for solving this problem: Shockley's depletion layer theory, Sah's approximation, and a numerical solution of Eqs. (1).

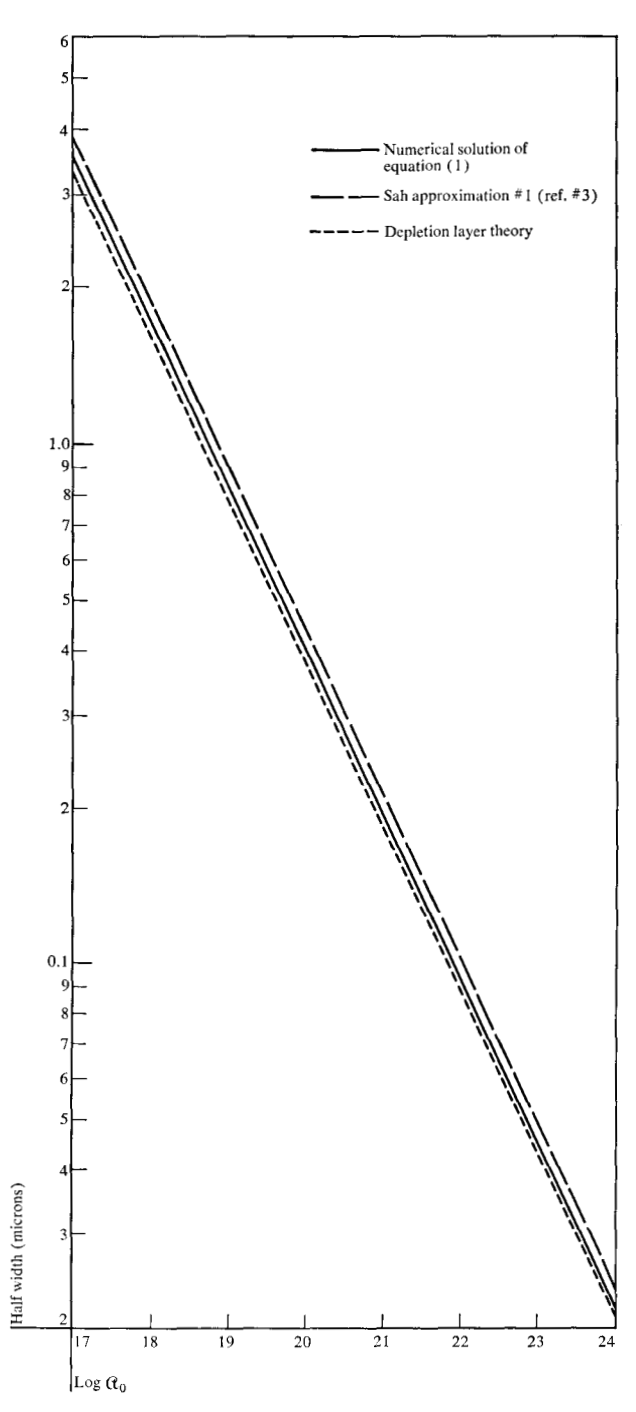
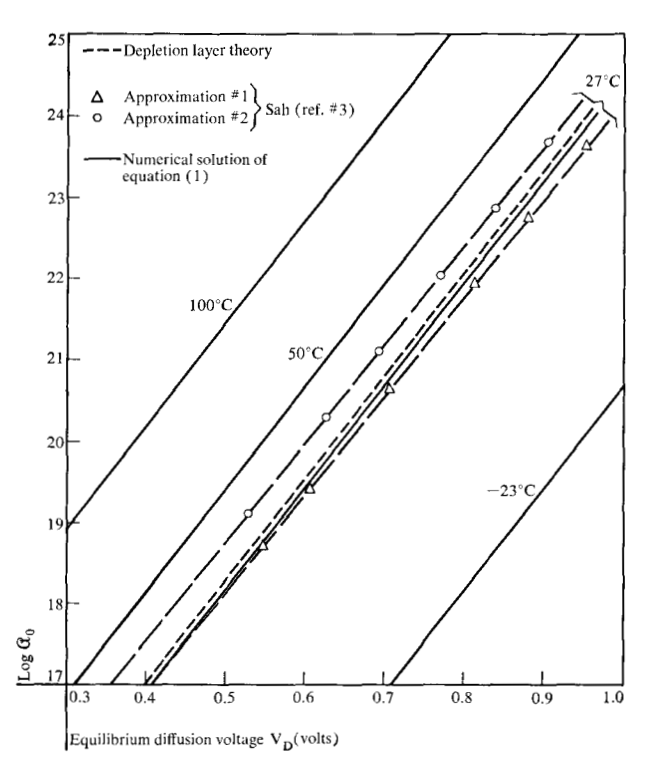


Figure 5 Equilibrium space-charge layer width in a linearly-graded p-n junction.

Although these three analytical methods yield nearly the same magnitude, it is emphasized that the space-charge layer width is an arbitrarily defined parameter. Small modifications in the definition for space-charge layer termination could substantially change any (or all) of the solutions illustrated in Fig. 5.



**Figure 6** Equilibrium diffusion voltage for a linearly-graded *p-n* junction.

For a linearly-graded p-n junction, the equilibrium diffusion voltage  $V_D$  is also an arbitrarily defined parameter. This situation arises from an impurity atom gradient within the semiconductor material outside the p-n junction space-charge layer. At thermal equilibrium this semiconductor material contains sufficient electrostatic charge to generate a small electric field. The magnitude of this electric field is determined by the impurity atom gradient. At thermal equilibrium, the drift component imparted to mobile charge carriers (by this "built-in" electric field) must have the same magnitude (but in the opposite direction) as the diffusion component arising from the mobile charge carrier gradient. For this reason, the equilibrium diffusion voltage of a linearly-graded p-n junction will increase with an increase in the distance over which this voltage is determined.

In the present discussion, the equilibrium diffusion voltage  $V_D$  is defined as the total difference of potential between specified locations on each side of the structure, and these locations are established by the theoretical spacecharge layer width (Fig. 5). The calculated equilibrium diffusion voltage is illustrated in Fig. 6. In this illustration, it is shown that all three analytical methods (Shockley, Sah, and the present analysis) are in substantial agreement.

# The linearly-graded collector junction

The transistor cut-off frequency  $(f_t)$  is a widely accepted measure of its current gain-bandwidth product (a frequency at which the short circuit common-emitter current gain becomes unity). Theoretically,  $f_t$  should increase with an increase of collector current (at a given collector voltage), although some workers have shown substantial deviations from this theory.  $^{26-28}$  Above some critical value of collector current  $f_t$  is found to decrease with increasing collector current. Kirk's explanation  $^{20}$  for this experimential observation is based upon the existence of a current-dependent mobile carrier density within the space-charge layer of the collector junction.  $^{29}$ 

In his investigation Kirk recognized that minority carriers within the collector junction space-charge layer (due to a large collector current) cannot be considered negligible in comparison to the fixed charge density of that region. He established that large values of collector current result in a spatial displacement of the collector junction space-charge layer edge, and that this displacement is in a direction tending to increase the transistor base width. It is qualitatively shown that this increase of base width provides a partial explanation for the experimentally observed high current fall-off of  $f_t$ .

Kirk used an abrupt p-n junction to approximate the mechanisms encountered in a collector junction of mesa geometry. This, of course, is a crude approximation for the modern diffused transistor. Nevertheless his analysis yields important contributions to the design of diffused collector junctions. It is often observed that the electrical characteristics of a diffused junction lie between those of an abrupt and a linearly-graded structure. 30,31 For this reason, Kirk's analysis outlines an important part of the large-current mechanisms encountered in diffused collector junctions; additional mechanisms are established in the present analysis of a linearly-graded junction. Future investigations will probably show that the large-current characteristics of an abrupt and a linearly-graded collector junction can be combined to explain the large-current properties of a diffused collector junction.

In the present investigation, numerical solutions of the collector junction problem are accomplished by previously outlined techniques. Infinite minority carrier lifetimes  $(\tau_n \text{ and } \tau_p)$  are assumed in the differential equations used to describe the operation of this semiconductor structure. Such an assumption eliminates from the analytical model any electric current due to either recombination or generation within the space-charge layer and the adjacent semiconductor material. In addition, it is also assumed that the entire collector current arises from a single type of charge carrier (either holes or electrons), as would be encountered at the collector junction of a transistor containing a forward-biased emitter junction.

Important considerations in the analysis of a collector junction are the mechanisms influencing electron and hole mobility. Semiconductor materials containing a large impurity atom density are known to exhibit reduced hole and electron mobilities.32 Further, elementary aspects of lattice scattering theory show that the average drift velocity of conduction band electrons and valence band holes is proportional to an applied electric field, but this proportionality is not always encountered in a practical semiconductor device.8-13 For example, at large values of electric field the electron velocity appears nearly fieldindependent, and in this environment it is frequently suggested that electrons exhibit a terminal velocity. Qualitative theoretical investigations of this subject have led to a satisfactory phenomenological explanation for the large-field drift characteristics of holes and electrons.12 although we are presently unable to quantitatively establish carrier velocities by other than experimental means.

Throughout the present analysis, published values are used for the small-field drift mobilities of holes and electrons. At each node within a relaxation matrix, the mobilities of holes and electrons are adjusted in accordance with the impurity atom density characterizing the device under consideration.

The large-field electrical properties of silicon and germanium have not been established in an unqualified fashion. In 1951, Shockley<sup>12</sup> conducted theoretical investigations on this topic, as applied to germanium. He established that a large electric field could produce electron temperatures up to 4000°K when, in fact, the material retained a lattice temperature of 300°K. This increased electron temperature produces an increased energy loss to acoustical modes of lattice vibration; thereby, the electron velocity increases as the square root of the electric field. A further increase of electron temperature produces a transfer of electron energy to optical modes of lattice vibration. Theory predicts that this additional mechanism results in an electron velocity that is constant and independent of the electric field.

In conjunction with this theoretical study, Ryder and Shockley<sup>33</sup> experimentally verified that the large-field drift velocity of electrons in germanium is proportional to the square root of the electric field. They also established that a very large electric field produces a terminal electron velocity. Furthermore, in a later study of this question Ryder<sup>8</sup> established that holes and electrons exhibit a similar field-dependent drift mobility, and that this phenomenon could be observed in both silicon and germanium. Although a field-dependent velocity was obtained for both holes and electrons in germanium, only electron conduction in silicon was found to exhibit a terminal velocity. Ryder believed that holes in silicon could be made to exhibit a terminal velocity, if these holes were subjected to a sufficiently large electric field.

At a later time, Gunn<sup>10</sup> conducted similar investigations on the large-field electrical properties of *n*-type germanium. Although his experiments place doubt upon some details arising from Ryder's experiments, general agreement was obtained concerning the large field characteristics of electrons in germanium. Thereafter, Prior<sup>11</sup> conducted similar measurements upon silicon and germanium throughout a wide range of material resistivity and electric field. Prior's investigation showed that a terminal carrier velocity is a unique characteristic of *n*-type germanium, and neither *p*-type germanium nor *n*-type or *p*-type silicon exhibit this phenomenon.

Granted that the foregoing presents a rather inconclusive picture concerning large-field characteristics of mobile charge carriers in silicon and germanium, the assumption of a terminal carrier velocity has nevertheless become traditional in mathematical investigations of collector junction operation. <sup>20,34,35</sup> This assumption represents a convenient simplification, rather than an unqualified physical characteristic. Further experimental work appears necessary before positive statements can be made concerning the influence of a large electric field upon carrier mobility.

For purposes of consistency, the present analysis is based upon the published experimental results of Ryder. 8 From this information, approximate equations have been developed to describe the relation between hole or electron velocities and an associated electric field. These equations are used to generate a correction factor for the drift mobility of holes and electrons in all calculations pertaining to semiconductor devices containing a sufficiently large electric field.

In an *n-p-n* transistor, collector junction space-charge displacement is one consequence of a large collector current density. For many years it was implicitly assumed that the electron velocity becomes infinite in a collector junction space-charge layer; Matz<sup>29</sup> emphasized the inaccuracy of this assumption. The finite electron velocity throughout this region results in a collector junction spacecharge layer (at large current densities) that contains sufficient mobile electrons to modify the structure electrically. This situation is illustrated in Fig. 7. In this illustration, the applied reverse biasing voltage (10 volts) was selected to assure that electrons attain the terminal velocity experimentally determined by Ryder,<sup>8</sup> and that this terminal velocity is maintained throughout a large portion of the total space-charge layer.

In previous investigations of this subject, the mobile charge carrier velocity was assumed constant throughout an entire collector junction space-charge layer. Experimental uncertainties concerning this assumption make it important to consider situations where a terminal velocity characteristic does not exist. For example, it can be shown from Ryder's experimental data that many *n-p-n* transistors

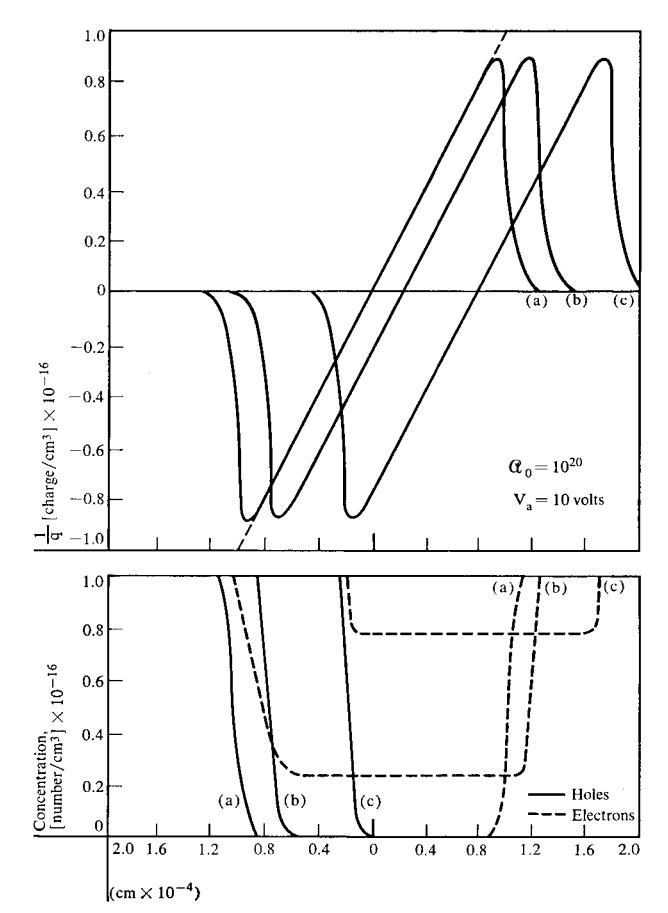
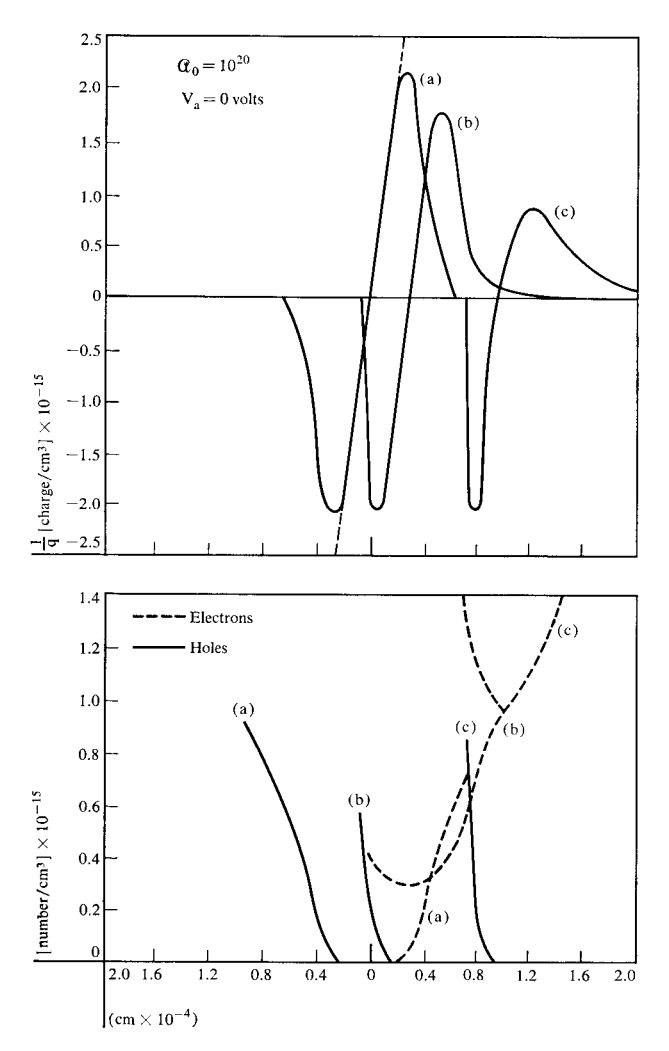


Figure 7 Calculated space-charge layer characteristics of a linearly-graded collector junction in a silicon n-p-n transistor: (a)  $J_c = 0$ ; (b)  $J_c = 3 \times 10^3$  amps/cm<sup>2</sup>; (c)  $J_c = 10^4$  amps/cm<sup>2</sup>.

require a substantial collector junction biasing voltage to attain the terminal electron velocity. In a low-voltage mode of collector junction operation, the electron velocity (and hence the electron density) is everywhere dependent upon the space-charge layer electric field. Regions containing a small electric field also contain a large electron density; this results in a non-uniform space-charge displacement, and hence substantial space-charge distortion.

Figure 8 illustrates such distortion. At a reasonable value of reverse biasing voltage the collector junction in Fig. 7 exhibits a nearly linear translation with an increase of collector current. In contrast, after removing the reverse biasing voltage (Fig. 8) this same collector junction undergoes substantial space-charge layer distortion.

At present, no experimental evidence is available to show that holes exhibit a terminal velocity in a silicon p-n junction. For this reason, space-charge layer distortion may be a fundamental characteristic of the collector junction in a p-n-p transistor. This situation is illustrated in Fig. 9, which presents calculated space-charge layer



**Figure 8** Calculated space-charge layer characteristics of a linearly-graded collector junction in a silicon *n-p-n* transistor: (a)  $J_c = 0$ ; (b)  $J_c = 3 \times 10^3$  amps/cm<sup>2</sup>; (c)  $J_c = 10^4$  amps/cm<sup>2</sup>.

characteristics for the junction shown in Fig. 7 (at the same reverse biasing voltage), except that the collector current is now assumed to arise from holes rather than electrons. Here we encounter the same basic type of distortion as that shown in Fig. 8, although Ryder's experiments imply that this distortion (Fig. 9) will exist at all values of collector junction biasing voltage.

These illustrative examples show that calculations of collector junction displacement are not necessarily a simple task, unless, of course, one can assume the existence of a terminal carrier velocity. For this reason, Fig. 10 presents detailed calculations establishing the linearly-graded collector junction displacement within both n-p-n and p-n-p transistors; this calculation is applicable over the range of collector current densities usually encountered in transistor operation ( $0 \le J_o \le 10^5$  amps/cm²). Again, it is emphasized that these calculations are based upon Ryder's

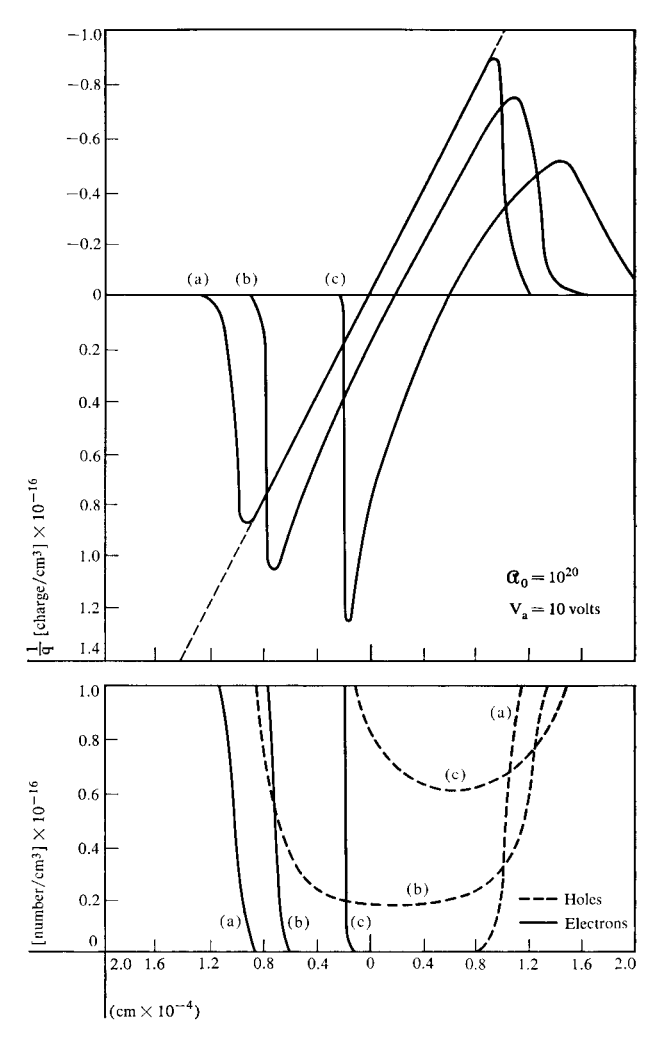


Figure 9 Calculated space-charge layer characteristics of a linearly-graded collector junction in a silicon p-n-p transistor: (a)  $J_c = 0$ ; (b)  $J_c = 3 \times 10^3$  amps/cm<sup>2</sup>; (c)  $J_c = 10^4$  amps/cm<sup>2</sup>.

measurements of the high field mobilities for holes and electrons, and that these measurements have been placed in question by other workers.

## The forward-biased junction

Previous investigations of the forward-biased, linearly-graded junction<sup>2,3</sup> were based upon a hypothetical model assumed free of minority carrier sources or sinks. This assumption implies that neither minority carrier generation nor recombination takes place within the device under consideration. In addition, this assumption implies that all ohmic contacts exhibit a recombination velocity of zero. A semiconductor structure of this type would have little practical value because no steady-state electric current could arise from the application of a forward biasing voltage. Initally, after applying a forward biasing voltage, a transient electric current could be observed at the *p-n* 

junction; given sufficient time, this electric current would decrease to zero and, thereafter, the structure would assume a state of quasi-equilibrium.

The state of quasi-equilibrium (forward-biased yet zero electric current) represents a situation where the mobile charge carrier densities (holes and electrons) are modified throughout an entire semiconductor device; the p-type material contains an excess of mobile electrons and, similarly, the *n*-type material contains an excess of holes. The magnitude of these excess carrier densities is accurately specified by the Boltzmann relations for a p-n junction. Because a space-charge can result from the introduction of excess minority carriers into otherwise charge neutral semiconductor material, an increase is also obtained in the density of majority carriers. Simultaneous with the injection of excess minority carriers by a forward-biased junction, a nearly equal quantity of majority carriers is introduced by the ohmic contacts; near charge neutrality is thereby maintained in the semiconductor material adjacent to a forward biased p-n junction.

It has been argued that mathematical investigations based upon a hypothetical zero-current model have limited applicability to practical semiconductor devices. This may (or may not) be true for most *p-n* junctions (abrupt, diffused, etc.). For the linearly-graded junction, however, inherent characteristics limit the electric current to a value substantially smaller than encountered in other types of structures. This limitation means that a forward-biased linearly-graded junction undergoes only small deviations from thermal equilibrium; it will therefore be shown that, for the linearly-graded junction, a zero-current model has little influence upon the applicability of the analysis.

First, let us consider the mathematical characteristics of this zero-current model of a forward-biased junction. From the Morgan and Smits analysis, Eq. (4a) can be rewritten into the form\*

$$\frac{d^2 U}{dy^2} = \frac{1}{K^2} (\sinh U - y), \tag{11}$$

where

$$y = \frac{\alpha_0 x}{2n_i} \exp\left(-q V_a/2kT\right), \tag{12a}$$

$$\mathcal{L}_D^2 = \kappa \epsilon_0 k T / 2q^2 n_i, \tag{12b}$$

$$K = K_0 \exp(-3q V_a/4kT)$$
, and (12c)

$$K_0 = \Omega_0 \mathcal{L}_D / 2n_i. \tag{12d}$$

It should be noted that when the applied junction voltage  $V_a$  is zero, Eq. (11) becomes identical to the equation (9) for a linearly-graded junction at equilibrium.

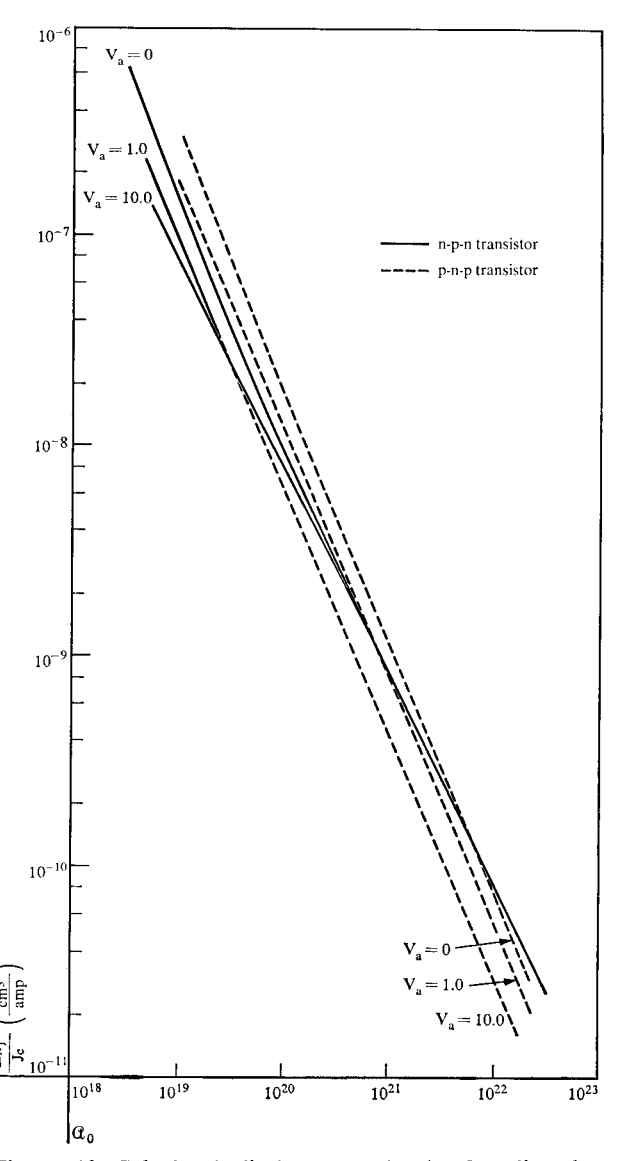


Figure 10 Calculated displacement  $(\Delta x_i)$  of a linearly-graded collector junction in silicon.

From (9) and (11), important similarities can be shown between a forward-biased junction and a junction at both potential and thermal equilibrium. For an equilibrium junction, Eq. (9) contains a characterizing dimensionless parameter  $K_0$ , the magnitude of which determines the degree of space-charge neutralization arising from mobile charge carriers. Similarly, for a forward-biased junction, Eq. (11),  $K_0$  is replaced by a dimensionless parameter K, and the magnitude of this parameter is determined by both  $K_0$  and the applied junction biasing voltage in Eq. (12c). Therefore, it is not surprising that a forward-biased linearly-graded junction exhibits many physical properties that were previously shown for an equilibrium junction of small impurity atom gradient.

<sup>\*</sup> This mathematical form is attributed to J. L. Moll by S. P. Morgan and F. M. Smits (see Ref. 3).

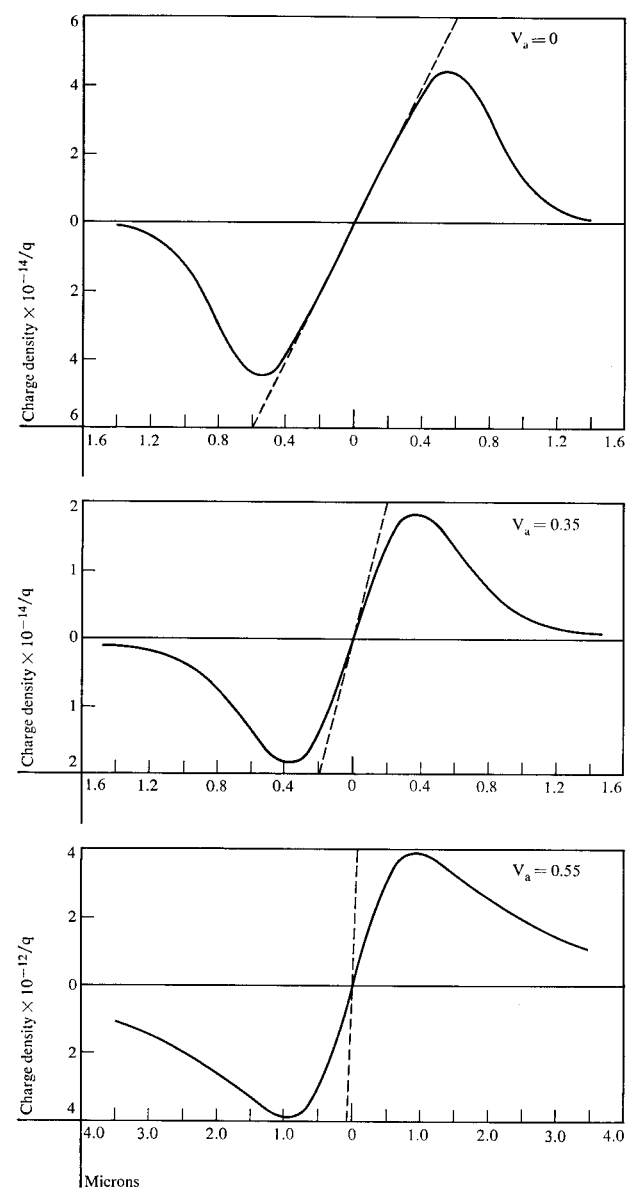


Figure 11 Space-charge characteristics of a forward-biased linearly-graded p-n junction (silicon). ( $a_0 = 10^{19}$  atoms/cm<sup>4</sup>.)

For example, consider the equilibrium p-n junction calculations shown in Fig. 1. At small values of impurity atom gradient, this illustration shows (in conjunction with Fig. 3) that the space-charge layer contains sufficient majority carriers (electrons within the n-type material and holes within the p-type material) to partially neutralize the electrostatic charge arising from ionized impurity atoms. In similar fashion, the forward-biased linearly-graded junction (Fig. 11) exhibits space-charge layer neutralization, and the degree of this neutralization is determined by both the impurity atom gradient  $\alpha_0$  and the forward biasing voltage  $V_a$ .

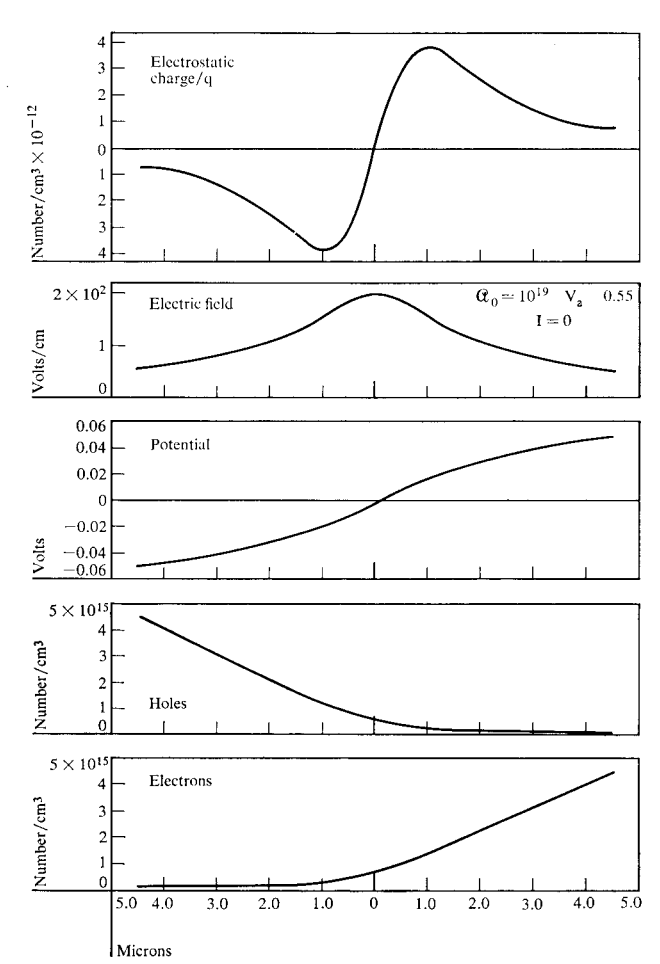


Figure 12 Space-charge layer characteristics of a forward-biased, linearly-graded p-n junction (silicon).

Figure 12 provides further evidence of similarities between an equilibrium junction containing a small impurity atom gradient (Fig. 3) and a forward-biased junction. Figure 12 shows that the calculated space-charge layer of a forward-biased junction contains large quantities of holes and electrons. These mobile charge carriers appear as majority carriers (holes within the *p*-type material and electrons within the *n*-type material), and for this reason we obtain substantial neutralization of the electrostatic charge arising from ionized impurity atoms. An important consequence of this mechanism is that in a forward-biased linearly-graded junction, the electrostatic charge density is everywhere appreciably less than the ionized impurity atom density.

Using previous definitions of the space-charge layer boundaries, Fig. 13 presents one-half the calculated space-charge layer width of a forward-biased, linearly-graded junction. Illustrated in this figure are the calculations from three different methods for solving the linearly-graded junction problem: a traditional extension of Shockley's

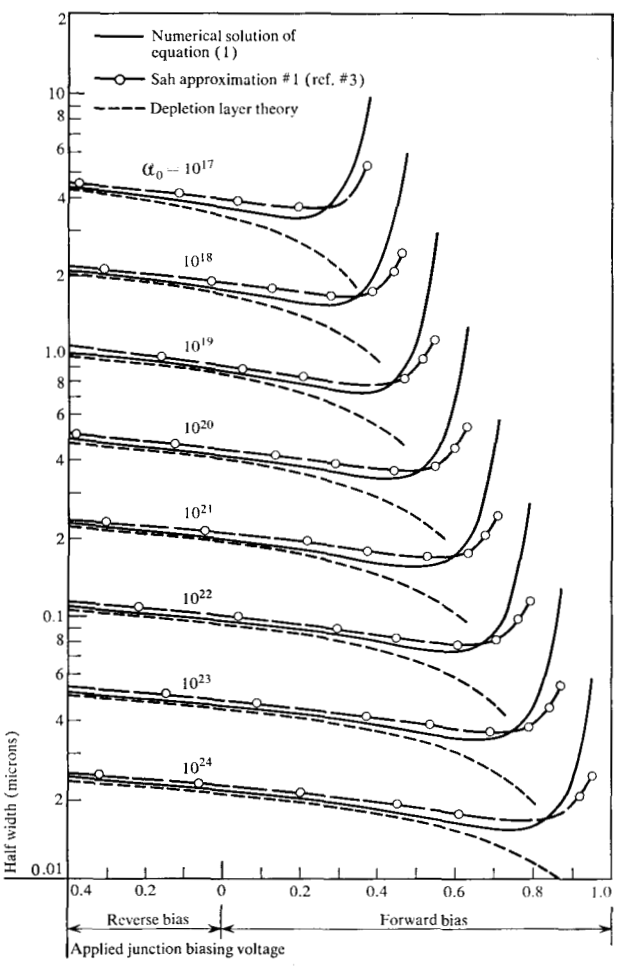


Figure 13 Space-charge layer width within a linearly-graded p-n junction (silicon).

theory, Sah's approximation, and a numerical solution of Eqs. (1). At small values of forward biasing voltage, the difference between these three analytical methods is negligible; the space-charge layer width decreases with an increase of forward biasing voltage. At large values of forward biasing voltage, however, a large increase of space-charge layer width results from a comparatively small increase of biasing voltage. This modification in junction operation is clearly a result of space-charge neutralization arising from majority carriers within each side of the structure under consideration.

As previously stated, this particular series of calculations (Fig. 13) is based upon an analytical model in which no steady-state electric current is permitted. To establish the consequences of this simplification, similar calculations were performed upon models containing hole current, electron current, and an equal quantity of both hole current and electron current. In these computations an infinite minority carrier lifetime was always maintained, and the electric current was attained by mathematically

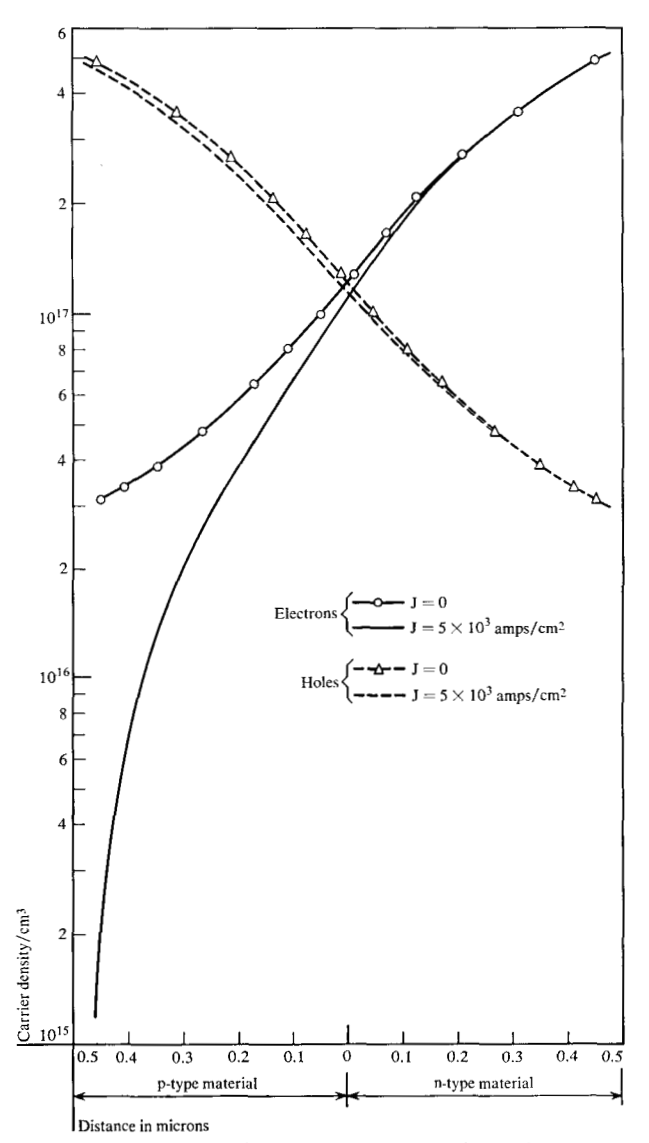


Figure 14 Hole and electron distribution within the space-charge layer of a linearly-graded p-n junction (silicon).

locating a minority carrier sink in the immediate vicinity of the p-n junction space-charge layer. In this fashion, by locating a sink in either the n-type or the p-type material, an electric current would arise from either holes or electrons, respectively. If, instead, sinks were located on both sides of the junction, an electric current would arise from both holes and electrons.

This series of calculations (non-zero electric current) was performed for p-n junctions throughout a wide range of impurity atom gradients  $\alpha_0$ , throughout a large variation of the forward biasing voltage, and at many different values of electric current. The results of these calculations can be outlined by a single statement: An exceedingly large value of current density is required to induce only minor deviations from the zero-current model.

An example of such a calculation is illustrated in Fig. 14.

In this figure, it can be observed that an electron current density of  $5 \times 10^3$  amps/cm<sup>2</sup> results in a factor-of-10 (approx.) decrease in the electron (minority carrier) density at the *p*-type space-charge layer edge, and a change of the same absolute magnitude in the hole density (majority carrier) at this location.

Previous discussions have established that majority (not minority) carriers have the greater influence upon the space-charge distribution within a forward-biased linearlygraded p-n junction. Figure 14 also illustrates a mechanism encountered in all forward-biased junction calculations: the introduction of an electric current has only a minor influence upon the majority carrier distribution in both p-type and n-type material. For this reason, it is concluded that the zero-current model of a forward-biased linearlygraded junction provides an adequate characterization of the space-charge distribution at large values of electric current. Although this approximation can introduce error in the calculated minority carrier density (up to a factor of 10 at the space-charge layer edge), the influence of this error upon most of electrical properties of the structure is very small.

# Space-charge layer capacitance

The depletion layer concept of p-n junction operation is based upon an assumption that the electrostatic charge density is everywhere equal to the density of ionized impurity atoms; therefore the space-charge region is completely depleted of mobile holes and electrons. In this structure the mechanisms contributing to electrical capacitance are similar to the mechanisms encountered within a parallel plate capacitor. From classical electrostatics,  $^{36,37}$  the electrical capacitance is given by

$$C = \frac{1}{V_T} \left( \frac{dW}{dV_T} \right) , \tag{13}$$

where  $V_T$  is the total difference of electrostatic potential across the region under consideration, and W is the electrostatic energy

$$W = \frac{\kappa \epsilon_0}{2} \int_{x_n}^{x_p} E^2(x) \ dx. \tag{14}$$

In Eq. (14), the parameter E(x) is the electric field distribution, and  $(x_p, x_n)$  are defined boundaries for the space-charge region.

For a reverse-biased linearly-graded junction, this classical equation for electrical capacitance is in substantial agreement with the depletion layer theory. Such agreement implies an essential mechanism contributing to the spacecharge layer electrical capacitance during this mode of junction operation: an increase in applied biasing voltage results in an increase in electrostatic energy. Despite the relatively crude depletion layer approximation for a *p-n* junction space-charge region (Fig. 4), this approximation

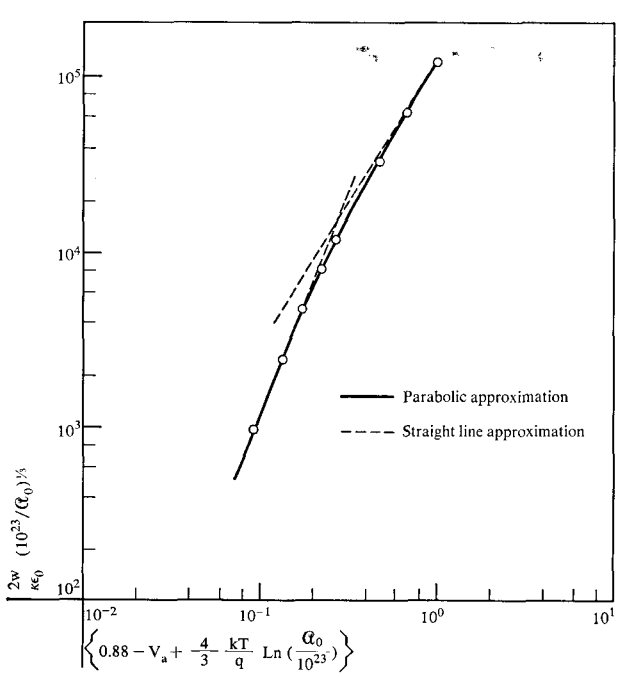


Figure 15 Calculated electrostatic energy in the space-charge layer of a linearly-graded junction (silicon).

is nevertheless adequate for electrical capacitance calculations. Furthermore, the depletion layer theory provides a degree of mathematical simplicity not obtainable in more rigorous computations of p-n junction capacitance.

Morgan and Smits<sup>2</sup> have established that electrostatic energy storage is important also in the operation of a forward-biased linearly-graded *p-n* junction. Through a manipulation of the integrated hole density equation for this semiconductor device, Morgan and Smits have shown two mechanisms contributing to the electrical capacitance: a storage of electrostatic energy (space-charge capacitance), and a storage of excess minority carriers (neutral capacitance),

$$C = q \frac{d}{dV} \int_{-\ell}^{\ell} p(x) dx$$

$$= 2q \frac{d}{dV} \int_{0}^{\ell} p(x) dx - \frac{d}{dV} \int_{0}^{\ell} \rho(x) dx, \qquad (15)$$

where  $\ell$  is a defined mathematical boundary of the structure. From this analysis, electrostatic energy storage arises from the same mechanism encountered in a reverse-biased p-n junction: a change of applied biasing voltage alters the electrostatic charge resulting from ionized donor and acceptor atoms. In contrast, Morgan and Smits classified excess minority carrier storage as a charge neutral process because the electrostatic charge arising from minority carriers is almost completely neutralized by excess majority carriers<sup>38</sup> (conductivity modulation).

Figure 15 illustrates the computed electrostatic energy W within the space-charge layer of a linearly-graded junction. Because this calculation was for junctions of arbitrary impurity atom gradient and applied biasing voltage, the parameters in Fig. 15 are given in a generalized form. If Fig. 15 is applied to a practical linearly-graded p-n junction (for example, to a junction containing an impurity atom gradient  $\alpha_0$  of  $10^{23}$ ), the applied biasing voltage  $V_a$  ranges from about 0.4 volts in the reverse (low current) direction, to a forward biasing voltage nearly equal to the equilibrium junction diffusion voltage.

The calculations illustrated in Fig. 15 were conducted with an assumed electric current of zero, even at large values of forward biasing voltage. To determine the consequences of this simplification, numerous values of electrostatic energy were calculated at current densities up to nearly 10<sup>4</sup> amps/cm<sup>2</sup>; at no time did a significant change arise from large values of electric current density. This observation is consistent with other calculations pertaining to the influence of an electric current upon the junction space-charge layer. The electrostatic charge distribution in a forward-biased junction is determined by the density of majority carriers within the space-charge layer, and these majority carriers are little influenced by the presence of an electric current.

From Fig. 15, an extension of the depletion layer approximation provides a satisfactory method for calculating the space-charge layer electrostatic energy at moderate values of forward biasing voltage. In contrast, at large values of forward biasing voltage this depletion layer concept is not applicable; the space-charge layer becomes densely populated with mobile charge carriers, and these carriers have a significant influence upon the total electrostatic energy. The biasing voltage at which this transition takes place depends upon the junction impurity atom gradient, and for this reason a simple, generally applicable rule cannot be stated. Instead, a "rule-of-thumb" important to device engineering is stated: at operating levels yielding a significant electric current, the space-charge layer can be assumed to contain a large quantity of mobile charge

At small values of forward biasing voltage, the electrostatic energy within a linearly-graded p-n junction can be approximated by the empirical formula

$$W = \alpha_1 V_T^{5/3}, \tag{16}$$

where  $V_T$  is the total junction voltage (both diffusion and applied) and  $\alpha_1$  is a constant of proportionality.

At large values of forward biasing voltage, majority carriers within the junction space-charge layer result in an electrostatic energy approximated by the empirical formula

$$W = \alpha_0 V_T^{5/2}, (17)$$

where  $\alpha_2$  is a constant of proportionality. Although the two approximation equations (16) and (17) exhibit a discontinuous transition between the large and small bias modes of junction operation, detailed calculations of this region (Fig. 15) show that a smooth transition actually exists.

From the approximation of (16) and (17), in conjunction with (13), the capacitance of this semiconductor structure is given by

$$C \simeq \beta_1 V_T^{-1/3},\tag{18}$$

at small values of forward biasing voltage. Further, at large values of forward biasing voltage this same spacecharge capacitance is

$$C \simeq \beta_2 V_T^{1/2}. \tag{19}$$

From these approximation equations, at small values of forward biasing voltage the space-charge capacitance of this junction increases (with an increase of voltage) until the structure becomes dominated by mobile charge carriers; a further increase of forward biasing voltage results in a decrease of space-charge capacitance.

From these electrostatic energy calculations (Fig. 15) a parabolic approximation equation was used to obtain a smooth transition between the two modes of junction operation: large and small values of forward biasing voltage. Thereafter this approximation equation, in conjunction with (13), was used to establish the space-charge layer capacitance arising from electrostatic energy storage.

A direct comparison has been made between the electrical capacitance component obtained from these electrostatic energy calculations (Fig. 15) and the space-charge capacitance calculations of Morgan and Smits. Substantial agreement is obtained at small values of forward biasing voltage (throughout the region where negligible charge neutralization arises from majority carriers within the junction space-charge layer). At large values of forward biasing voltage Fig. 15 yields an electrical capacitance of approximately one-half the value determined by Morgan and Smits. It has been established that the principal differences between these two calculations are the assumed mathematical boundaries of the problem.

In the Morgan and Smits calculation, mathematical boundaries are located on each side of the p-n junction space-charge region, and the separation between these boundaries is assumed sufficient to maintain a difference of potential of  $20 \ kT/q$  ( $\approx 0.5 \ \text{volts}$ ). Boundaries of this type are used by Morgan and Smits in all computations of junction capacitance, even for devices operating at large values of forward biasing voltage. A consequence of this assumption is easily seen by its application to a forward-biased junction. For example, consider a linearly-graded junction containing an impurity atom gradient  $\alpha_0$  of  $10^{24}$  atoms/cm. An external forward biasing voltage of

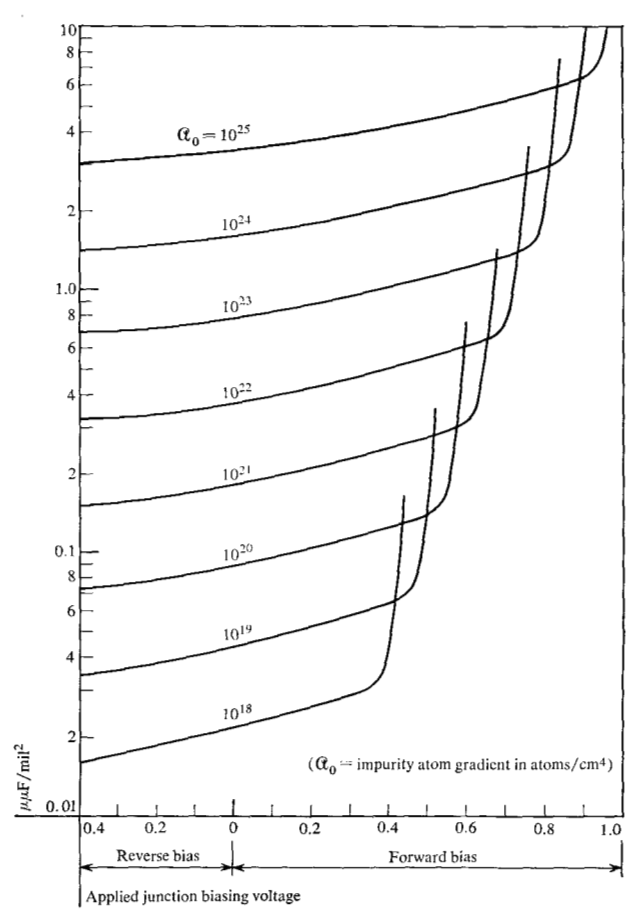


Figure 16 Space-charge layer capacitance of a linearly-graded p-n junction (silicon). ( $\alpha_0 = \text{impurity atom gradient in atoms/cm}^4$ .)

0.885 volts would locate the mathematical boundaries at approximately 125 microns on each side of the junction, while the total space-charge layer width is only 0.04 microns.

From this example it is apparent that the Morgan and Smits calculation of space-charge capacitance includes substantial semiconductor material outside the junction space-charge layer. If this extra semiconductor material is charge neutral or if, instead, this material contains a space-charge that is totally independent of the junction biasing voltage, the boundaries used by Morgan and Smits have no influence upon the calculated capacitance. Neither requirement is satisfied in a calculation of space-charge capacitance for a forward-biased junction. Minority carrier injection, in association with conductivity modulation, yields a space-charge density that is small when compared with the density of excess minority carriers, yet this space-charge is sufficient to modify the theoretical space-charge capacitance at large values of forward biasing voltage. In contrast, the capacitance determined from Fig. 15 in conjunction with Eq. (13) results only from spacecharge layer electrostatic energy, and not from the electrostatic energy of minority carrier storage; the magnitude of this capacitance is therefore smaller than the value calculated by Morgan and Smits.

In addition to space-charge neutralization, minority carrier storage contributes significantly to the electrical capacitance of a forward-biased junction. Detailed calculations of this mechanism show that a forward biased linearly-graded junction stores excess minority carriers within both the *p-n* junction space-charge layer and the adjacent semiconductor material. Neglecting the time constant associated with increasing and decreasing this large quantity of excess minority carriers (thereby implying a low frequency), minority carrier storage appears as a capacitance (sometimes called a diffusion capacitance) when viewed at the external terminals of the device.

Throughout the present investigation, minority carrier storage capacitance was derived from calculations of excess minority carriers within the space-charge layer of a forward-biased linearly-graded junction. These calculations were performed for a wide range of biasing voltage, and thereafter graphic techniques were used to determine the rate at which this quantity of excess carriers changes with applied voltage; this derivative represents the carrier storage capacitance.

Figure 16 illustrates the total calculated low-frequency electrical capacitance exhibited by the space-charge region within a linearly-graded junction. This total is composed of both the capacitance arising from an energy storage within the electrostatic field (space-charge capacitance) and the minority carrier storage within this same region (sometimes called the neutral capacitance or the diffusion capacitance).

Figure 16 shows two basically different regions in the capacitance characteristic of a forward-biased junction: a low-voltage region that exhibits a small increase of capacitance with voltage, and a high-voltage region (biasing voltage nearly equal the equilitrium junction diffusion voltage) where the capacitance increases rapidly with voltage. The low-voltage capacitance is established by electrostatic energy storage within the space-charge layer, and the magnitude of this capacitance is determined by Fig. 15 in conjunction with Eq. (13). At large values of biasing voltage, an increased capacitance arises from minority carrier storage. It is emphasized that any minority carrier storage process is a function of both frequency and electric current; Fig. 16 represents the low-frequency and zero-current capacitance. Similar calculations have been conducted for junctions at large electric current densities (up to 10<sup>4</sup> amps/cm<sup>2</sup>). Such calculations show that Fig. 16 illustrates the maximum minority carrier storage capacitance for a p-n junction space-charge layer; a large electric current density can reduce this capacitance component to one-half its zero-current magnitude.

For purposes of comparison, Fig. 17 illustrates the theoretical electrical capacitance of a forward-biased, linearly-graded p-n junction, as derived from the analysis of Morgan and Smits, Sah, and from Fig. 16. This calculation is based upon an assumed impurity atom gradient of  $10^{24}$  atoms/cm<sup>4</sup>, and an electric current of zero.

Figure 17 shows that at small values of forward biasing voltage, substantial agreement exists between these three computations of electrical capacitance. In contrast, at large values of forward biasing voltage  $(0.6 < V_a)$  unsatisfactory agreement is obtained; yet this particular range of forward biasing voltage is the one most frequently used in semiconductor device operation. Because electrical capacitance is an important property of p-n junctions, the disagreement illustrated in Fig. 17 has been investigated. Resulting from this investigation is an understanding of the source of disagreement, and some inherent limitations upon the applicability of each mathematical computation of p-n junction electrical capacitance.

As in their computation of space-charge capacitance, the stored charge capacitance (neutral capacitance) calculations of Morgan and Smits were conducted upon an analytical model of unusually large physical dimensions. For example, at an applied junction biasing voltage of 0.6 volts in Fig. 17, Morgan and Smits calculated the stored minority carriers within a region of 0.37 microns on each side of the space-charge layer (the space-charge layer width is 0.032 microns). Similarly, at an applied biasing voltage of 0.86 volts this region increased to 59 microns on each side of the structure (the space-charge layer width is 0.036 microns). If, instead, the Morgan and Smits computation is restricted to the space-charge layer of this junction (Fig. 13), agreement is obtained with the computations illustrated in Fig. 16.

Sah's computation of junction capacitance is derived from a mathematical model in substantial agreement with the model used for Fig. 16. The principal difference between Sah's calculation and Fig. 16 lies in the approximation methods used. Unless this boundary problem is solved in a rigorous fashion, small errors arising from an approximate solution lead to significant quantitative errors in a computation of the complicated electrical parameters associated with a *p-n* junction.

It is important to consider the applicability and utility of linearly-graded-junction theory in the field of semi-conductor device design. From a practical point of view, few laboratory techniques presently exist whereby a truly linearly-graded junction can be fabricated. For this reason, the principal usefulness of linearly-graded-junction theory arises from an assumption that this structure is a simplified mathematical approximation for a diffused *p-n* junction. Such an assumption appears reasonable if the approximation is limited to the junction space-charge layer; throughout this region a linearly-graded impurity profile

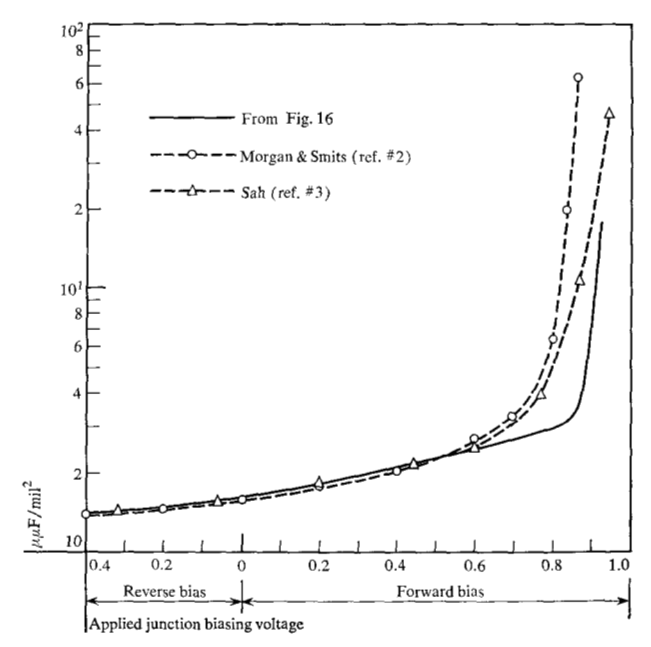


Figure 17 Electrical capacitance of a linearly-graded p-n junction (silicon) ( $\alpha_0 = 10^{24} \text{ atoms/cm}^4$ ).

is often (but not always) a satisfactory first approximation for a diffused impurity atom profile. If, instead, the linearly-graded model is applied to regions of a diffused junction far removed from the space-charge layer, significant analytical errors could result from an unwise application of this simplified model.

The principal difference between Fig. 16 and the Morgan and Smits analysis is the magnitude of minority carrier storage capacitance resulting from a given forward biasing voltage. Figure 16 represents the electrical capacitance attributable to a linearly-graded junction space-charge layer; only this portion of the capacitance is assumed to be a reasonable approximation for the mechanisms encountered in a diffused p-n junction. In contrast, the capacitance computations of Morgan and Smits include minority carrier storage within the semiconductor material adjacent to the junction space-charge layer, and the length of this region is often equal to (or greater than) the material thicknesses used in device fabrication. For diffused semiconductor devices, it is proposed that minority carrier storage outside a p-n junction space-charge layer is seldom approximated by similar storage mechanisms within a linearly-graded junction.

Figure 16 indicates that the design of linearly-graded junctions can be optimized to yield a minimum space-charge layer capacitance. At a given forward biasing voltage, a large electrical capacitance is obtained for devices containing an excessively small impurity atom gradient; this capacitance is due to excess minority carrier storage within the junction space-charge layer. Similarly, at this

same biasing voltage an excessively large impurity atom gradient also results in a large electrical capacitance; this capacitance is due to electrostatic mechanisms within the space-charge layer. Between these two limiting conditions, a minimum space-charge layer capacitance is encountered at a specific impurity atom gradient; the particular gradient yielding this minimum capacitance is presumed to be optimum for the particular biasing voltage under consideration.

### References

- 1. W. Shockley, B.S.T.J. 28, 436 (1949).
- 2. S. P. Morgan and F. M. Smits, B.S.T.J. 39, 1573 (1960).
- 3. C. T. Sah, Proc. IRE 49, 603 (1961).
- R. E. Bellman and R. E. Kalaba, Quasilinearization and Nonlinear Boundary Value Problems, American Elsevier Publishing Co., New York, 1965.
- E. A. Coddington and N. Levinson, Theory of Ordinary Differential Equations, McGraw-Hill Book Co., Inc., New York, 1955.
- 6. W. Van Roosbroeck, B.S.T.J. 29, 560 (1950).
- 7. S. Chandrasekhar, Rev. Mod. Phys. 15, 1 (1943).
- 8. E. J. Ryder, Phys. Rev. 90, 766 (1953).
- 9. M. B. Prince, Phys. Rev. 92, 681 (1953); 93, 1204 (1954).
- 10. J. B. Gunn J. Elect. & Ctrl. 2, 87 (1956).
- 11. A. C. Prior, J. Phys. Chem. Solids 12, 175 (1959).
- 12. W. Shockley, B.S.T.J. 30, 990 (1951).
- 13. K. B. Wolfstirn, J. Phys. Chem. Solids 16, 279 (1960).
- C. T. Sah, R. N. Noyce and W. Shockley, *Proc. IRE* 45, 1228 (1957); see also Ref. 1.
- R. V. Southwell, Relaxation Methods in Engineering Science, Oxford Univ. Press, London, 1940.
- R. V. Southwell, Relaxation Methods in Theoretical Physics, Vol. I, Oxford Univ. Press, London, 1946.

- R. V. Southwell, Relaxation Methods in Theoretical Physics, Vol. II, Oxford Univ. Press, London, 1956.
- R. V. Southwell, An Introduction to the Theory of Elasticity, Oxford Univ. Press, London, 1941.
- G. E. Forsythe and W. R. Wasow, Finite-Difference Methods for Partial Differential Equations, John Wiley and Sons, New York, 1960.
- 20. C. T. Kirk, IRE Trans. ED-9, 164 (1962).
- W. E. Milne, Numerical Solution of Differential Equations, John Wiley and Sons, New York, 1953.
- 22. W. Schottky, Z. Physik 113, 367 (1939); 118, 539 (1942).
- W. Schottky and E. Spenke, Wiss Veröffentl a.d. Siemens-Werken 18, 3 (1939).
- 24. N. F. Mott, Proc. Roy. Soc. (London) A171, 27 (1939).
- H. S. Harned and B. B. Owen, The Physical Chemistry of Electrolytic Solutions, Third Edition, Reinhold Publishing Co., New York, 1958.
- 26. R. L. Pritchard, Proc. IRE 46, 1152 (1958).
- 27. C. Thornton and J. Angell, Proc. IRE 46, 116 (1958).
- 28. M. Clark, Proc. IRE 46, 1185 (1958).
- 29. A Matz, J. Elect. and Ctrl. 7, 133 (1959).
- 30. R. M. Scarlett, IRE Trans. ED-6, 405 (1959).
- D. P. Kennedy and R. R. O'Brien, IRE Trans. ED-9, 478 (1962).
- 32. W. Shockley, *Electrons and Holes in Semiconductors*, D. Van Nostrand, New York, 1950.
- 33. E. J. Ryder and W. Shockley, Phys. Rev. 81, 139 (1951).
- 34. R. D. Middlebrook, Solid-State Electronics 6, 555 (1963).
- 35. R. D. Middlebrook, Solid-State Electronics 6, 573 (1963).
- W. R. Smythe, Static and Dynamic Electricity, McGraw-Hill Book Co. Inc., New York, 1950.
- 37. G. P. Harnwell, Principles of Electricity and Electromagnetism, McGraw-Hill Book Co. Inc., New York, 1938.
- 38. W. M. Webster, Proc. IRE 42, 914 (1954).

Received October 21, 1966.